Interaction of Myosin Subfragment 1 with Fluorescent Ribose-Modified Nucleotides. A Comparison of Vanadate Trapping and SH_1–SH_2 Cross-Linking†

Christine R. Cremo,*,‡ Joan M. Neuron,§ and Ralph G. Yount§

Department of Chemistry, The Colorado College, Colorado Springs, Colorado 80903, and Biochemistry/Biophysics Program, Institute of Biological Chemistry, and Department of Chemistry, Washington State University, Pullman, Washington 99164-4660

Received October 6, 1989

ABSTRACT: The environment near the ribose binding site of skeletal myosin subfragment 1 (S1) was investigated by use of two adenosine 5′-diphosphate analogues with fluorescent groups attached at the 2′- and 3′-hydroxyls of the ribose ring. We have compared steady-state and time-resolved fluorescent properties of the reversibly bound S1–nucleotide complexes and the complexes generated by *N,N′-p*-phenylenedimaleimide (pPDM) thiol cross-linking or vanadate (V_i) trapping. A new fluorscent probe, 2′(3′)-*O*-[*N*-[2-[[[5-(dimethylamino)naphthyl]sulfonyl]amino]ethyl]carbamoyl]adenosine 5′-diphosphate (DEDA-ADP), which contains a base-stable carbamoyl linkage between the ribose ring and the fluorescent dansyl group, was synthesized and characterized. For comparison, we performed parallel experiments with 2′(3′)-*O*-(*N*-methylanthraniloyl)adenosine 5′-diphosphate (MANT-ADP) [Hiratsuka, T. (1983) *Biochim. Biophys. Acta 742*, 496–508]. Solute quenching studies indicated that both analogues bound reversibly to a single cleft or pocket near the ribose binding site. However, steady-state polarization measurements indicated that the probes were not rigidly bound to the protein. The quantum yields of both fluorophores were higher for the complexes formed after trapping with pPDM or V_i than for the reversibly bound complexes. Both DEDA-ADP and MANT-ADP, respectively, had nearly homogeneous lifetimes free in solution (3.65 and 4.65 ns), reversibly bound to S1 (12.8 and 8.6 ns), and trapped on S1 by pPDM (12.7 and 8.7 ns) or V_i (12.8 and 8.6 ns). In contrast to the quantum yields, the lifetimes were not increased upon trapping, compared to those of the reversibly bound states. These results suggested that static quenching in the reversibly bound complex was relieved upon trapping. Taken together, the results suggest that there was a conformational change near the ribose binding site upon trapping by either pPDM or V_i. On the basis of the quantum yield, lifetime, polarization, and solute accessibility studies, we could not detect differences between the S1–pPDM–nucleotide analog complex and the S1–V_i–nucleotide analogue complex for either analogue. Thus, previously observed differences with the adenine modified nucleotide analogue 1,N^6-ethenoadenosine diphosphate (ϵADP) could not be detected with these ribose-modified probes, indicating that structural differences may be localized to the adenine binding site and not transmitted to the region near the ribose ring.

The recent discovery that only the isolated heads of myosin, S1,[1] are necessary for movement on actin filaments (Yano-Toyoshima et al., 1987; Kishino & Yanagida, 1988; Chaen et al., 1989) has focused increased attention on the nature of the ATP binding site on S1. This site and the actin binding site(s), with which it interacts, must be key elements in any contractile mechanism. Kinetic studies have provided considerable insight into the mechanism of the hydrolysis of ATP by S1 and acto–S1 [for reviews, see Taylor (1979), Adelstein and Eisenberg (1980), and Hibberd and Trentham (1986)]. To study the structural changes implied in the proposed actomyosin–adenosinetriphosphatase (ATPase) mechanisms, it is of interest to characterize long-lived analogues of intermediates in the ATPase pathway. To date, two stable nucleotide–myosin complexes, M·pPDM·ADP and $M^{\dagger}$·ADP·V_i, have been studied and evaluated as candidates for analogues of such intermediates.

Reisler et al. (1974) have shown that treating S1 with the thiol cross-linker pPDM in the presence of nucleotide completely inactivates the enzyme. Since then, it has been shown that pPDM cross-links the reactive thiols SH_1 (Cys-707) and SH_2 (Cys-697) (Burke & Knight, 1980; Huston et al., 1988), trapping the nucleotide stably and noncovalently at the active site (Wells & Yount, 1979, 1982). pPDM cross-linking favors an S1 conformation whose circular dichroism spectrum resembles that of the enzyme during steady-state hydrolysis (Burke et al., 1976). Greene et al. (1986) showed that acting binding promoted the rapid loss of ADP from the S1·

† This work was supported by Grant DK-05195 from the National Institutes of Health and by the Muscular Dystrophy Association. The Varian 2200 spectrophotometer used in these studies was purchased with funds provided by NSF Equipment Grant PCM-8400841.

‡ The Colorado College.

§ Washington State University.

[1] Abbreviations: S1, myosin subfragment 1; V_i, orthovanadate; pPDM, *N,N′-p*-phenylenedimaleimide; M·pPDM·MgADP, the stable complex consisting of MgADP bound to myosin (M) that has been cross-linked by the bifunctional thiol cross-linking reagent pPDM; $M^{\dagger}$·MgADP·V_i, the stable complex formed slowly after association of the ternary complex consisting of myosin, MgADP, and V_i, where $M^{\dagger}$ indicates a conformationally altered myosin; DMF, dimethylformamide; TLC, thin-layer chromatography; MANT-ADP, 2′(3′)-*O*-(*N*-methylanthraniloyl)adenosine 5′-diphosphate; dansyl, 5-(dimethylamino)-naphthalene-1-sulfonate and its derivatives; DEDA, 5-(dimethylamino)-*N*-(2-aminoethyl)naphthalene-1-sulfonamide; DEDA-ADP, 2′(3′)-*O*-[*N*-[2-[[[5-(dimethylamino)naphthyl]sulfonyl]amino]ethyl]carbamoyl]adenosine 5′-diphosphate; ADP-CC, adenosine 5′-diphosphate 2′,3′-cyclic carbonate; TEA, triethylamine; TEAB, triethylammonium bicarbonate; ϵADP, 1,N^6-ethenoadenosine 5′-diphosphate; Bz_2ADP, 3′(2′)-*O*-(4-benzoylbenzoyl)adenosine 5′-diphosphate; $Bz_2\epsilon$ADP, 3′(2′)-*O*-(4-benzoylbenzoyl)-1,N^6-ethenoadenosine 5′-diphosphate.

0006-2960/90/0429-3309$02.50/0

pPDM·ADP complex and that pPDM cross-linked S1 bound to actin with an affinity similar to that of S1 in the presence of ATP. As would be expected for an analogue of S1·ATP or S1·ADP·P_i, the binding is several orders of magnitude weaker than that of S1·ADP, S1 alone, or S1·AMPPNP, regardless of which nucleotide is bound to S1·pPDM (Greene et al., 1986). Cross-linking of the two thiols, not just alkylation, appears to be necessary for locking-in a conformation that mimics the steady-state intermediates, S1·ATP or S1·ADP·P_i (Burke et al., 1976).

The other analogue of intermediates in the ATPase pathway is formed by ADP and orthovanadate, which together bind stoichiometrically at the active site of myosin to form an inactive stable complex, $M^{\dagger}$·ADP·V_i (Goodno, 1979, 1982). Vanadate is a phosphate analogue that can adopt a stable trigonal-bipyrimidal geometry that is believed to be the geometry of the γ-PO_4 of ATP during hydrolysis of ATP to ADP and P_i. For this reason, the proposal that $M^{\dagger}$·ADP·P_i is a stable analogue of the predominant steady-state intermediate of the ATPase pathway (M^{**}·ADP·P_i) has been tested by several different methods. Spectroscopic evidence is limited as the enhanced tryptophan fluorescence of the M^{**}·ADP·P_i complex cannot be detected in the comparable $M^{\dagger}$·ADP·V_i complex due to Förster energy transfer between tryptophan and V_i itself. However, the mobility of a spin probe on myosin SH_1 (Wells & Bagshaw, 1984) and the tryptic digestion pattern of HMM (Ajtai et al., 1982) in the $M^{\dagger}$·ADP·V_i complex are similar to those seen during steady-state ATPase activity. As with S1·pPDM·ADP, actin destabilizes the $M^{\dagger}$·ADP·V_i complex. $M^{\dagger}$·ADP·V_i binds to actin with about one-tenth the affinity of S1·ADP·P_i (Goodno & Taylor, 1982).

Fluorescence has proven to be a valuable tool for examining the structural differences between various intermediates and their stably trapped analogues. In particular, ϵADP, an adenine-modified nucleotide analogue (Secrist et al., 1972; Leonard, 1984), has been extensively studied, as it is trapped in the same manner as ADP by both pPDM (Perkins et al., 1984) and V_i (Rosenfeld & Taylor, 1984; Aguirre et al., 1989). In agreement with tryptophan fluorescence studies (Trybus & Taylor, 1982), the fluorescence properties of S1·ϵADP and S1·ϵATP indicate at least two bound nucleotide states that are in equilibrium (Rosenfeld & Taylor, 1984; Aguirre et al., 1989). The effect of vanadate upon the S1·ϵADP complex is to increase the rotational mobility (Aguirre et al., 1989) and decrease the accessibility to solute quenching (Rosenfeld & Taylor, 1984) of the ethenoadenine ring and to decrease the distance between ϵADP and the divalent metal binding site (Aguirre et al., 1989). In contrast, pPDM cross-linking of SH_1 and SH_2 does not alter the orientation or mobility and has essentially no effect upon the solvent accessibility of ϵADP bound to S1 (Perkins et al., 1984). Thus, by probing of the adenine binding site, the pPDM-cross-linked and the V_i-trapped states are found to be structurally different. These two stable analogues may then resemble different intermediates in the myosin–ATPase pathway.

In the present study, we have used two ribose-modified fluorescent nucleotide derivatives to probe the region of S1 near the ribose binding site for structural differences between the pPDM-cross-linked and the V_i-trapped states. We have synthesized DEDA-ADP by reacting the 2′,3′-cyclic carbonate of ADP (Maeda et al., 1977) with DEDA to form a new fluorescent analogue with a base-stable carbamoyl linkage. This synthetic approach (Neuron et al., 1988; Braxton & Yount, 1988) promises to be of general use in preparing nucleotide derivatives that are more base stable than the commonly used ester derivatives. We have compared the fluorescence properties of DEDA-ADP to those of the previously synthesized MANT-ADP (Hiratsuka, 1983, 1984a,b). We found only slight differences between the reversibly bound and trapped complexes and virtually no difference for either analogue between the S1·pPDM·nucleotide complex and the S1·V_i·nucleotide complex, indicating that the two trapped states are indistinguishable with respect to the region near the ribose binding site. These probes, having been fully characterized bound at the active site, are now good candidates for fluorescence resonance energy transfer studies involving the active site of myosin and other nucleotide binding proteins.

Materials and Methods

The sources of commercial compounds were as follows: disodium (or dilithium) adenosine 5′-diphosphate and 5′-triphosphate (Pharmacia P-L Biochemicals); 100 atom % D_2O (Aldrich); ultrapure guanidine hydrochloride (Schwarz/Mann); chymotrypsin, *Escherichia coli* alkaline phosphatase (EC 3.1.3.1), quinine sulfate, carbonyldiimidazole, dansyl chloride, DEAE-Sephadex A-25-120, Sephadex G-50-80, phenylmethanesulfonyl fluoride, and chymotrypsin (Sigma); *N*,*N*′-*p*-phenylenedimaleimide, recrystallized from chloroform and stored at 1 mM in acetonitrile at −20 °C (Aldrich); *N*-methylisatoic anhydride (Molecular Probes); analytical TLC plates 60 F254 (EM Science); sodium orthovanadate (Na_3VO_4; Fischer); glycerol, MB grade (Boerhinger Mannheim). TEAB solutions were prepared as described by Mahmood et al. (1987). Stock vanadate solutions (100 mM at pH 10) were prepared as described by Goodno (1982) and stored on ice. Total and acid-labile phosphate were analyzed as described by Lanzetta et al. (1979) with ATP and K_2HPO_4 (Baker) as standards. Dimethylformamide (DMF) was dried by vacuum distillation from tosyl chloride and was stored over 4-Å molecular sieves. Triethylamine (Baker) was redistilled and stored at 4 °C. Tributylamine (Pierce) was stored at 4 °C. Carbonyldiimidazole was dried under vacuum over phosphorus pentoxide.

ATPase assays were performed as described previously (Wells et al., 1979b), except that release of inorganic phosphate was measured at 2 and 8 min after the addition of S1 to the assay mixture. Protein concentrations were measured by the Coomassie blue dye binding method of Bradford (1976) with unmodified S1 as a standard, as previously described (Wells et al., 1979a).

Protein Preparation. Myosin was isolated from rabbit leg and back muscles as previously described (Wagner & Yount, 1975) and stored in 50% glycerol at −20 °C. Chymotryptic S1 (115 000 g/mol, $\epsilon_{280}^{1\%} = 7.5$ cm^{-1}) was prepared as described by Okamoto and Sekine (1985) with the following modifications: the myosin was dialyzed overnight into 0.12 M NaCl–10 mM sodium phosphate (pH 7.0 at 25 °C) and made 1 mM in EDTA just prior to addition of chymotrypsin; the ammonium sulfate precipitated protein was resuspended in S1 buffer containing 0.7 mg/mL phenylmethanesulfonyl fluoride prior to gel filtration. This latter step was required to inactivate traces of chymotrypsin, which slowly reactivates after PMSF treatment. S1 was stored on ice in 0.1 M KCl, 50 mM Tris, and 0.025% NaN_3, adjusted to pH 8.0 at 0 °C (S1 buffer), and used within 2 weeks.

Enzyme Inactivations. Fluorescent nucleotide analogues were stably trapped at the active site of S1 by either V_i by pPDM in the following manner (unless otherwise indicated): S1 (17 μM) in S1 buffer was equilibrated at 25 °C for 10 min with a 2 molar excess of fluorescent nucleotide analogue and 2 mM $MgCl_2$. Inactivation by V_i was initiated by addition

Scheme I: Synthesis of 2′(3′)-*O*-[*N*-[2-[[[5-(Dimethylamino)naphthyl]sulfonyl]amino]ethyl]carbamoyl]adenosine 5′-Diphosphate[a]

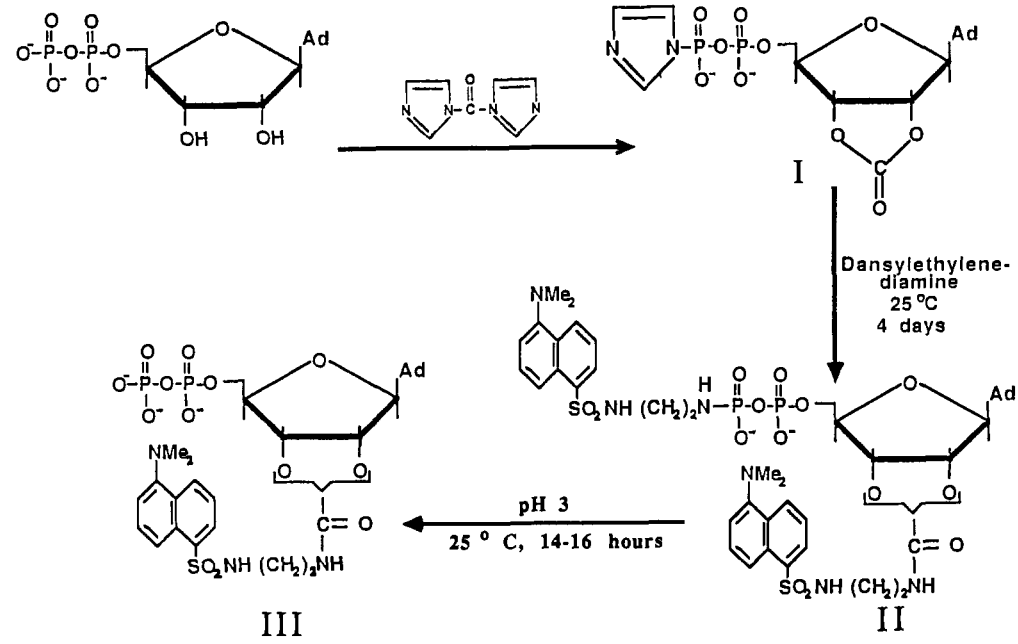

[a] The phosphoryl imidazolidate of ADP 2′,3′-cyclic carbonate (I) was prepared from ADP and CDI as described under Materials and Methods. Subsequent reaction with DEDA produced didansylated ADP (II). The phosphoramide bond was cleaved by acid to form the final product: 2′(3′)-*O*-[*N*-[2-[[[5-(dimethylamino)naphthyl] sulfonyl]amino]ethyl]carbamoyl]-ADP (III).

of V_i to a final concentration of 1 mM (Goodno, 1982). The reaction was quenched after 20–30 min at 25 °C by addition of EDTA to 20 mM, followed by a 50-fold excess of ATP (over binding sites) to reduce nonspecific binding of fluorescent nucleotide to the protein. Inactivation with pPDM was initiated by addition of a 1.1-fold excess of pPDM over S1 as described by Wells et al. (1979). The reaction was quenched after 20 min at 0 °C by addition of a 200-fold excess of β-mercaptoethanol over S1, followed by the addition of EDTA and ATP as described above. The S1–nucleotide complex was separated from untrapped nucleotide and trapping agent by centrifugal gel filtration (Penefsky, 1977) over Sephadex G-50-80 equilibrated in S1 buffer.

The concentrations of nucleotide analogues in trapped and purified S1 samples were determined by the fluorescence intensity in 4.5 M guanidine hydrochloride, pH 8.0, with excitation at 366 nm and emission monitored at 446 nm (MANT-ADP) or 552 nm (DEDA-ADP).

Steady-state fluorescence measurements were made with an SLM 4800 fluorometer (SLM Instruments, Urbana, IL), interfaced with a Hewlett-Packard 9825A computer and 7224A plotter. The excitation was at 366 nm for all measurements. Emission spectra were taken at 6 °C with the excitation polarizer (calcite prism) set at 55° from vertical and the emission polarizer at 0°. Excitation and emission slit widths were set at 4 nm for MANT-ADP and 16 nm for DEDA-ADP. Correction factors were obtained by calibrating the emission monochromator and photomultiplier with a standard tungsten light source. Intensity fluctuations of the xenon lamp and variations in the efficiency of the excitation monochromator were corrected by use of a rhodamine B quantum counter in the reference detector. All solutions were filtered through a Millex-PF 0.8-μm filter to minimize light scattering. Fluorescence quantum yields were calculated relative to quinine sulfate in 0.1 N H_2SO_4 as described by Parker and Reese (1960). A red-sensitive photomultiplier tube (Hamamatsu R-928) was used for DEDA-ADP measurements. A Varian 2200 UV–visible spectrophotometer was used to measure absorbance in 3-mL quartz cuvettes.

Steady-state polarization measurements were made with calcite prism polarizers and were corrected by subtracting out polarization emission intensity contributions from light scattering of an appropriate blank at each polarizer setting. The polarization values were obtained at 4 °C by exciting the sample at 366 nm and measuring the emission intensity through a Schott 408 nm cutoff filter.

Lifetime measurements were made with a home-built multifrequency and phase-modulation fluorometer based on the Gratton design (Gratton & Limkeman, 1983; Gratton et al., 1984). Excitation used the 364-nm line of an argon laser (Spectra Physics Model 2035-3.5S); emission was detected through a Schott OG 399 nm cutoff filter. The fluorescence lifetimes at 4 °C were calculated from the phase shift and demodulation of the sample-emitted light with respect to a glycogen standard. The modulation frequency was varied between 10 and 70 MHz at 10-MHz intervals. The data were fit to single- or double-exponential decays, and the χ_R^2 value was calculated with a constant, frequency-independent standard deviation of 0.2° and 0.004 for phase and modulation values, respectively.

Syntheses. MANT-ADP was synthesized by the method of Hiratsuka (1983). The synthesis of DEDA-ADP is described in Scheme I. The progress of all reactions was followed by TLC in solvent A [1-butanol/acetic acid/water (5:2:3)] or solvent B [isobutyric acid/ammonia/water (75:1:24)]. The phosphoryl imidazolidate of ADP-CC (I) was synthesized by a modification of the method of Maeda et al. (1977) as follows: A 3 × 10 cm column of Dowex 50W-X8 (Baker, triethylammonium form) was used to prepare the triethylammonium salt of ADP (1 mmol) from the dilithium salt. The ADP was then dried by rotary evaporation at 25 °C, 10 mmol of tributylamine was added, and the mixture was exhaustively dried by repeated rotary evaporation from dry DMF. Carbonyldiimidazole (4 mmol in 18 mL of DMF) was added, and the reaction mixture was stirred at 20 °C for 2 h, at which time the excess carbonyldiimidazole was quenched by the addition of 62 μL (1.52 mmol) of absolute methanol. The yield of the phosphoryl imidazolidate of ADP-CC (I) by

this method was nearly 100%, as determined by TLC (R_f values of 0.37 and 0.33 in solvents A and B, respectively). DEDA (ϵ^{M}_{325nm} = 4400 cm^{-1} M^{-1}) was synthesized by the method of DePecol and McCormick (1979) and stored in methanol at −20 °C. The free base of DEDA (1 mmol in 3 mL of DMF) and tributylamine (0.5 μmol) were added to 0.4 mmol of I in 15–18 mL of dry DMF, and the reaction was stirred at 25 °C for 4 days. H_2O (20 mL) was added, the pH was adjusted to 3.5 with glacial acetic acid (10.2 mL), and the mixture was stirred at 25 °C for 14–16 h to hydrolyze the phosphoramide of II (R_f values of 0.53 and 0.46 in solvents A and B, respectively) to give III. After evaporation, the residue was dissolved in a small volume of methanol, before addition of excess of 1 M NaI in acetone to precipitate the nucleotides as sodium salts. Unreacted DEDA was removed by repeated acetone washes (40 mL each) followed by low-speed centrifugation. The precipitate was dried under a stream of N_2, dissolved in 4 mL of H_2O, and applied to a 2.2 × 97 cm DEAE-Sephadex A-25 column (HCO_3^- form) equilibrated in H_2O at 4 °C. The flow rate was maintained at 3.5 mL/min with a peristaltic pump (Sigma), and 12-mL fractions were collected. Four major peaks of 259-nm absorbance were obtained upon elution with a linear gradient of 1 L each of H_2O and 0.6 M TEAB (pH 7.8). The composition of the peaks was identified by TLC in solvents A and B: AMP (R_f values of 0.32 and 0.34, minor peak) eluted at 0.3 M TEAB, ADP (R_f values of 0.08 and 0.2) and DEDA-AMP (R_f values of 0.54 and 0.56) coeluted at 0.4 M TEAB, and DEDA-ADP (R_f values of 0.43 and 0.45) eluted at 0.55 M TEAB. Residual unreacted DEDA (R_f values of 0.85 and 0.62) eluted in the void volume, and a minor unidentified fluorescent product eluted at 0.65 M TEAB (R_f values of 0.34 and 0.28). Compounds II and III, DEDA-AMP, and the unidentified fluorescent product(s) migrated as closely spaced but well-resolved doublets on TLC, corresponding to the 2′- and 3′-isomers (see ^{1}H NMR of Nucleotide Derivatives). The average R_f of each doublet is reported. The product peak was pooled, lyophilized, and stored in S1 buffer at −20 °C. The overall yield ranged from 10 to 30% for three syntheses.

^{1}H NMR of Nucleotide Derivatives. ^{1}H NMR spectra were measured on a Nicolet 200-MHz spectrometer at 4 °C. Proton assignments were based on coupling constants, comparison with standard spectra, and the knowledge that protons on the ribose ring which are attached to carbons carrying the electron-withdrawing fluorophores (e.g., $C_{3'}$, 3′-isomer) are found downfield of the signal for the same proton but of the other isomer (e.g., $C_{3'}$, 2′-isomer). The proton resonances are reported in ppm downfield from an internal standard of tetramethylsilane.

^{1}H NMR of MANT-ADP (sodium salt; 60% D_2O, 40% MeOD, pH 6.0, 11 mM; 1 mM EDTA added to chelate paramagnetic ions): δ 8.46 (s, 0.65 H, C_2, 3′-isomer), 8.42 (s, 0.34 H, C_2, 2′-isomer), 8.07 (s, 0.64 H, C_8, 3′-isomer), 8.00 (s, 0.33 H, C_8, 2′-isomer), 7.93 (dd, 0.67 H, *N*-methylanthraniloyl ring, ortho to carbamoyl linkage, 3′-isomer), 7.71 (dd, 0.36 H, *N*-methylanthraniloyl ring, ortho to carbamoyl linkage, 2′-isomer), 7.36–7.28 (m, 1.0 H, *N*-methylanthraniloyl ring, 3′- and 2′-isomers), 6.67–6.43 (m, 2.1 H, *N*-methylanthraniloyl ring, 3′- and 2′-isomers), 6.22 (d, 0.38 H, $C_{1'}$, 2′-isomer), 6.09 (d, 0.67 H, $C_{1'}$, 3′-isomer), 4.8–4.0 (br m, 2.0 H, $C_{5'}$, 2′- and 3′-isomers), 2.72 (s, 2.0 H, *N*-methyl, 3′-isomer), 2.64 (s, 1.0 H, *N*-methyl, 2′-isomer), 5.57–5.50 (m, 1.0 H, $C_{2'}$, 3′-isomer, and $C_{3'}$, 3′-isomer), 4.95–4.89 (dd, $C_{2'}$, 3′-isomer), 4.42–4.38 (br, $C_{4'}$, 3′-isomer), 4.35–4.24 (br, $C_{4'}$, 2′-isomer). Note that the nature of the signal of the $C_{3'}$ proton for the 2′-isomer and the integrations for the last three signals mentioned were obscured by the H_2O peak.

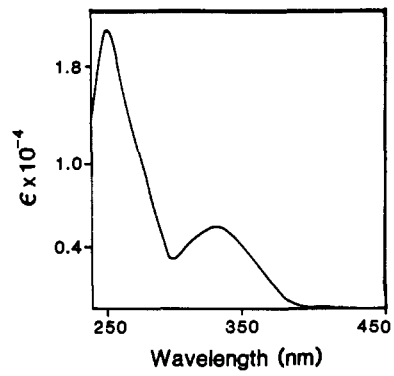

FIGURE 1: UV–visible absorption spectrum of DEDA-ADP.

^{1}H NMR for DEDA-ADP (sodium salt, D_2O, pH 6.0, 30 mM; EDTA added to 1 mM): δ 8.85–6.67 (m, 8.0 H, C_2, C_8, and all dansyl ring protons except for *N*-methyls), 5.93 (d, 0.34 H, $C_{1'}$, 2′-isomer), 5.82 (d, 0.66 H, $C_{1'}$, 3′-isomer), 5.14 (dd, 0.33 H, $C_{2'}$, 2′-isomer), 4.96 (dd, 0.66 H, $C_{3'}$, 3′-isomer), 4.54 (dd, 0.66 H, $C_{2'}$, 3′-isomer), 4.40 (dd, 0.33 H, $C_{3'}$, 2′-isomer), 4.2–3.95 (br m, 3.1 H, 2′- and 3′-isomers of both $C_{5'}$ and $C_{4'}$), 2.6–2.4 (br d, 4.5 H, ethylenediamine protons, both isomers). The signal for the *N*-methyl protons of the dansyl group was obscured under the signal for residual TEA at δ 2.9.

Results

Characterization of Nucleotide Analogues. The UV–visible absorption and fluorescence emission spectra of MANT-ADP (data not shown) were identical with those reported by Hiratsuka (1983). The ^{1}H NMR spectrum (see Materials and Methods) for MANT-ADP was consistent with the structure of a monosubstituted ribose-modified analogue, present as a mixture of the 2′-isomer (35%) and the 3′-isomer (65%).

The UV–visible spectrum of DEDA-ADP is shown in Figure 1. The peak at 330 nm was attributed to the DEDA moiety (Hudson & Weber, 1973). The molar extinction coefficient, ϵ^{M}_{330nm} = 4350 ± 60 cm^{-1} M^{-1}, was determined by total and acid-labile phosphate analysis (Lanzetta et al., 1979). The ^{1}H NMR spectrum (see Materials and Methods) for DEDA-ADP agreed with the proposed structure in Scheme I. The product was a mixture of 2′- and 3′-isomers in a ratio of 33:67, respectively. This result was consistent with the migration of the product as a well-resolved doublet on TLC.

Trapping of Nucleotide Analogues in the Presence of pPDM or V_i. To verify that the fluorescent nucleotide analogues were interacting specifically with the active site of S1, we compared their ability to promote V_i or pPDM inactivation of S1–NH_4^+ATPase activity with the parent nucleotide ADP. The time courses of inactivation of the nucleotide analogues with both trapping agents were essentially identical with that of ADP (data not shown). The parent fluorophores, methylanthranylic acid and DEDA, did not inactivate S1–ATPase under the trapping conditions.

As another measure of binding specificity, the stoichiometry of trapping by pPDM or V_i was determined by measuring the total fluorescence after denaturation of the purified and trapped complexes (Table I). Both derivatives were trapped nearly stoichiometrically at the active site by either method and were comparable to the trapping of ADP (between 80 and 90%). The trapping of both fluorescent derivatives was essentially zero when a 10-fold excess of MgADP over S1 was added to the solution prior to addition of Vi or pPDM (data not shown). These results indicated that the analogues were

Table I: Fluorescence Properties of Nucleotide Derivatives[a]

	MANT-ADP				DEDA-ADP			
property	free[f]	bound to S1[g]	V_i trapped[h]	pPDM trapped[h]	free[f]	bound to S1[g]	V_i trapped[h]	pPDM trapped[h]
quantum yield[b]	0.255 ± 0.003	0.57 ± 0.04	0.65 ± 0.02	0.64 ± 0.01	0.089 ± 0.001	0.252 ± 0.001	0.271 ± 0.003	0.29 ± 0.02
polarization[c]	0.044	0.416	0.412	0.412	0.043	0.365	0.375	0.370
lifetimes (ns)[d]	4.0	8.9	8.6	8.7	3.6	12.8	12.8	12.7
F_i	0.97	1.00	1.00	1.00	1.00	0.96	0.97	0.95
χ_R	2.85	0.96	0.90	0.93	1.02	5.85	5.29	9.95
% trapping[e]			90	85			91	88

[a] Absorbance at 366 nm was below 0.02 for all experiments. [b] Relative to quinine sulfate in 0.1 N H_2SO_4; quantum yield, 0.735 (6 °C). All values are the average and standard deviation of three independent experiments. [c] For conditions, see Materials and Methods. Each value is the average of triplicate measurements from three independent experiments (standard deviations were ±0.005 on all measurements). [d] For conditions, see Materials and Methods. Analyses were performed at 4 °C in S1 buffer. F_i is the fractional fluorescence intensity, and χ_R^2 (Jameson et al., 1984) is a reflection of the goodness of a fit to a single- or double-exponential model. [e] Expressed as the percent of S1 containing trapped nucleotide, determined as described under Materials and Methods. [f] 4 μM MANT-ADP or 8 μM DEDA-ADP in S1 buffer. [g] As described in Figure 3. [h] Trapped and purified as described under Materials and Methods.

trapped specifically at the active site by pPDM and V_i.

As a first step in our investigation of the fluorescence properties of the ribose-modified probes, we monitored the fluorescence intensity changes during trapping to verify that these effects were correlated to the loss of NH_4^+ATPase activity. Figure 2A shows the time course of a representative experiment with MANT-ADP using pPDM as the trapping agent. For the first 10 min of the experiment, the fluorophore was free in S1 buffer in the presence or absence of pPDM. The fluorescence of the control without pPDM was typically 5% higher than that of the sample containing pPDM, due to an inner-filter effect caused by pPDM absorption at 366 nm. The fluorescence intensity of the samples remained constant until the indicated times (arrows), when S1 was added to both the control and the sample containing pPDM. The instantaneous increase in fluorescence intensity was due to reversible binding of the fluorophore to the active site of S1. After this point, the fluorescence intensity of the control remained constant. However, in the presence of pPDM there was a slow, time-dependent increase in the fluorescence intensity due to trapping of MANT-ADP at the active site. The same experiment was done with DEDA-ADP. The fluorescence intensity changes associated with the trapping of MANT-ADP and DEDA-ADP by pPDM are shown in panels B and C of Figure 2, respectively. In these plots, the initial rapid increase in fluorescence intensity due to reversible binding (determined from the control: 130% for MANT-ADP; 220% for DEDA-ADP) was subtracted from the time-dependent increase to obtain the percent increase in intensity due only to trapping. The decrease in NH_4^+ATPase activity over this time course was plotted to show the linear correlation between trapping and fluorescence intensity changes (Figure 2B,C, insets). The fluorescence changes due to binding and trapping were not observed in the absence of $MgCl_2$ or in the presence of a 10-fold excess of MgADP (data not shown). We also observed time-dependent changes in fluorescence intensity for both probes upon trapping with 0.4 mM V_i, which were correlated to the decrease in NH_4^+ATPase activity (data not shown). The maximal fluorescence intensity of MANT-ADP trapped with V_i was 6% greater than that of MANT-ADP reversibly bound, while the comparable fluorescence intensity of DEDA-ADP trapped with V_i decreased by 11%. These changes in fluorescence intensity were inconsistent with the quantum yields of the trapped and purified complexes subsequently determined (see below). These discrepancies were attributed to an inner-filter effect caused by the large V_i concentrations necessary for convenient trapping times and by a possible quenching of the trapped complexes by binding of excess V_i to sites other than the active site.

Emission Spectra and Quantum Yields. It was of interest to further quantitate the fluorescence changes upon binding and trapping by directly measuring the quantum yields. The corrected emission spectra of free, reversibly bound, V_i-trapped, and pPDM-trapped analogues are shown in Figure 3. The spectra of the buffer or unmodified S1 were subtracted as appropriate. V_i- or pPDM-trapped S1·MgADP samples were purified and diluted to the same protein concentration to serve as blanks for the trapped samples. These spectra reflect changes in the quantum yields upon reversible binding and trapping because all samples were adjusted to the same absorbance at the excitation wavelength. For the reversibly bound samples, greater than 95% of the probe was bound to S1, on the basis of the binding constants determined by equilibrium dialysis for MANT-ADP or by polarization measurements for DEDA-ADP (data not shown, see Discussion). The emission maximum of MANT-ADP shifts from 447 nm when free in solution to 442 nm when reversibly bound to S1. The spectrum of DEDA-ADP also showed a blue shift from 578 nm when free in solution to 548 nm when reversibly bound on S1. Although the spectra of both analogues exhibited an increase in quantum yield upon trapping, only the MANT-ADP spectrum showed an additional blue shift (to 440 nm when trapped with pPDM and to 439 nm when trapped with V_i).

The quantum yields calculated from the spectra in Figure 3 are summarized in Table I. The reversible binding of MANT-ADP to S1 increased the quantum yield by 124%, with a further increase of 14% when trapped with pPDM or V_i. The quantum yield of DEDA-ADP increased by 183% when reversibly bound, with a further increase of 11% when trapped with V_i or pPDM. For MANT-ADP, these results were consistent with the maximal fluorscence intensity changes observed during the trapping time course with pPDM (Figure 2A,B). The small differences between the results of these two experiments can be attributed to the different experimental conditions.

Lifetimes. As the quantum yields of both MANT-ADP and the DEDA-ADP increased upon trapping, it was possible that the reversibly bound complexes were more statically quenched by the protein than the trapped complexes. To test for this, we measured the singlet lifetimes, which are not sensitive to static quenching. The lifetimes of both probes were nearly homogeneous under all conditions (Table I). For those samples with fractional fluorescence intensities less than 1.0, the residual intensity was due to a lifetime component corresponding to the free fluorophore or a small scattered light component. The lifetimes of both probes increased upon reversible binding to S1: by a factor of 2 for MANT-ADP and by a factor of

Table II: Stern–Volmer Quenching Constants (M^{-1}) of Nucleotide Derivatives[a]

	MANT-ADP				DEDA-ADP			
quencher	free	bound to S1	V_i trapped	pPDM trapped	free	bound to S1	V_i trapped	pPDM trapped
acrylamide	2.43 ± 0.01	0.20 ± 0.03	0.12 ± 0.02	0.18 ± 0.02	−0.42 ± 0.04	0.12 ± 0.02	0.09 ± 0.02	0.05 ± 0.01
KI	1.46 ± 0.01	0.84 ± 0.03	0.61 ± 0.03	0.70 ± 0.03	0.50 ± 0.03	0.88 ± 0.03	0.75 ± 0.03	0.75 ± 0.03
CsCl	0.002 ± 0.001	0.005 ± 0.001	0.04 ± 0.02	0.03 ± 0.02	0.15 ± 0.02	0.38 ± 0.02	0.20 ± 0.03	0.20 ± 0.03

[a] Aliquots were taken from 5 M aqueous stock solutions. The iodide solution contained 10^{-4} M sodium thiosulfate to prevent oxidation of I^- to I_3^-. Complete mixing of the quenching agent was assured by continuous magnetic stirring of the solution in the fluorescence cuvette. Emission was measured through a 389 nm cutoff filter with λ_{ex} = 366 nm. The conditions for the free, reversibly bound, and trapped complexes were as described in Figure 3. The slope of the plot of F_0/F vs quencher concentration (from 0 to 0.4 M), where F_0 and F are the fluorescence intensities in the absence and presence of quencher, respectively, was determined by linear regression analysis to give the Stern–Volmer quenching constant. The errors in the Stern–Volmer constants were estimated by assuming a 1.5% error in all fluorescence readings.

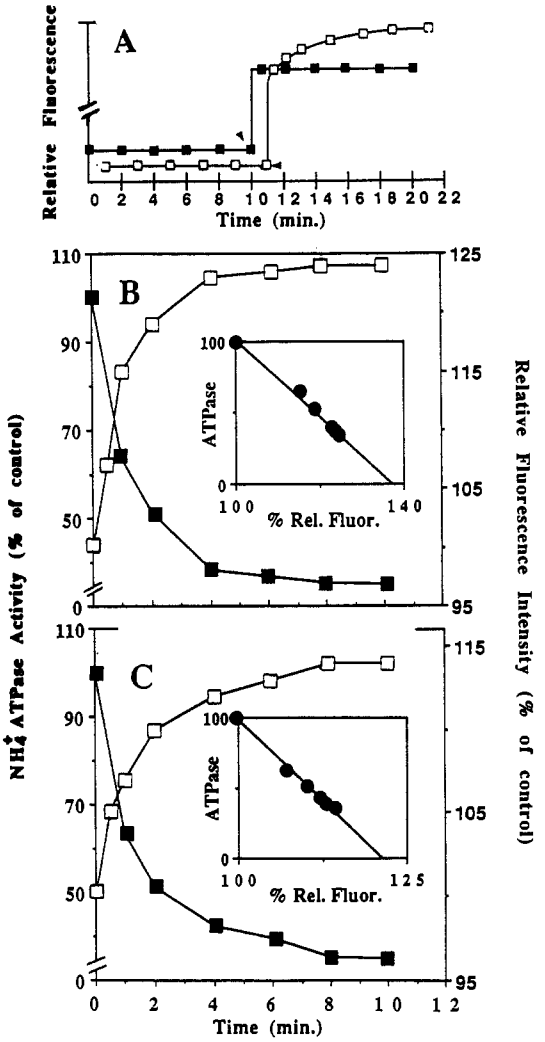

FIGURE 2: Fluorescence intensity vs inactivation by pPDM. Fluorescence intensity changes that occur during inactivation of S1-NH_4^+ATPase activity by pPDM in the presence of MANT-ADP (A and B) or DEDA-ADP (C). 5 μM nucleotide in S1 buffer was equilibrated with 2 mM $MgCl_2$ in the presence [A–C, (□)] or absence [A (■)] of 8.8 μM pPDM for 30 min at 0 °C. Solutions were placed in 3-mL cuvettes and incubated in the fluorometer at 6 °C for 10 min. Samples were excited at 366 nm with a 4-nm band-pass, and the fluorescence intensity was montiored through a 389 nm cutoff filter. Photobleaching of the sample was minimized by continuous magnetic stirring. At the indicated times (panel A, arrows), concentrated S1 (150–200 μM) was added to a final concentration of 8 μM, the fluorescence intensity was measured, and aliquots were removed and quenched with β-mercaptoethanol. NH_4^+ATPase activities [B and C, (■)] were determined within 2 h. All values are expressed as the percent of a control to which no pPDM was added. The NH_4^+ATPase activity was plotted versus relative fluorescence intensity (see insets).

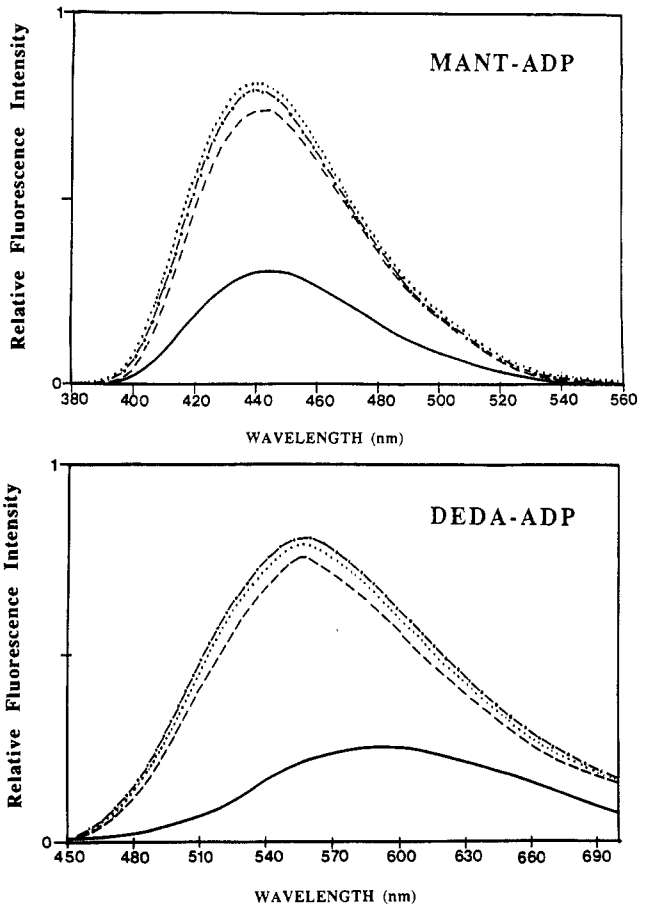

FIGURE 3: Molecular fluorescence emission spectra of nucleotide analogues. For conditions, see Materials and Methods. All solutions were diluted such that the absorbance at 366 nm was 0.02. MANT-ADP or DEDA-ADP in S1 buffer (—); MANT-ADP or DEDA-ADP reversibly bound to S1, 2 mM $MgCl_2$, nucleotide/S1 ≤ 0.1 such that greater than 90% of the nucleotide was found (– –); trapped complexes, purified as described under Materials and Methods, V_i (···) or pPDM (–·–).

3.5 for DEDA-ADP. However, there was no further detectable increase in the lifetime of either fluorophore upon trapping. Therefore, the process of trapping increases the quantum yield but not the lifetimes, suggesting that some static quenching of the fluorophore was relieved upon trapping.

Polarization. The changes in mobility of the fluorophores upon reversible binding to S1 and after trapping with V_i and pPDM were measured by steady-state polarization (Table I). The mobility of both probes decreased upon reversibly binding to the active site. However, the polarization values for the trapped complexes were not significantly different from those for the reversibly bound complexes for either probe.

Solute Quenching. The accessibility of the fluorophores to solute quenchers was compared under various conditions by calculation of Stern–Volmer quenching constants (Stern & Volmer, 1919; Table II) from plots of relative fluorescence versus quencher concentration. Within the range of acryl-

amide, KI, and CsCl concentrations studied, the data for all samples could be described by a straight line (correlation coefficients >0.95 by linear least-squares regression), indicating the absence of multiple components or a significant level of static quenching. Although acrylamide and KI were found to be effective quenchers of MANT-ADP, the CsCl quenching constants were too low to provide useful information. Upon binding to S1, the Stern–Volmer constants decreased significantly for both acrylamide (92%) and KI (43%), although the accessibility cannot be directly compared due to the spectral shifts (see Figure 2). Upon trapping with either pPDM or V_i, there was a further small decrease in the Stern–Volmer constants. However, considering the uncertainties in the measurement of these small constants, there was essentially no meaningful difference between bound and trapped values for either KI or acrylamide. For DEDA-ADP free in buffer, only the ionic quenchers, KI and CsCl, quenched, whereas the nonionic quencher, acrylamide, caused an increase in fluorescence. There was no significant difference between the accessibility of DEDA-ADP to all three quenchers in the reversibly bound form or in the two different trapped forms. Thus, for all quenchers tested, trapping did not cause any apparent change in the accessibility of either fluorophore.

Discussion

The primary goal in these studies was to use fluorophores attached to ADP to probe the region near the ribose binding site of myosin. Our earlier photolabeling studies (Mahmood et al., 1987, 1989) have shown that the photoreactive carboxybenzophenone group on the ribose of Bz_2ADP specifically photolabels Ser-324 in the 50-kDa heavy-chain tryptic peptide. Because all the labeling was associated with only one amino acid, the implication was that the hydrophobic benzophenone group bound specifically to one site. In addition, Sutoh (1987) has recently given evidence that a nitrophenyl azide group attached to the 2′(3′)-hydroxyls of an ADP derivative photolabels a hydrophobic region near Trp-130 in the 23-kDa NH_2-terminal tryptic peptide of the heavy chain. In addition, Szilagyi et al. (1979) have reported that a ribose-linked ATP photoaffinity analogue also labels the 23-kDa peptide. Thus it appears reasonable that the region near where the ribose ring binds includes elements of both the 23- and 50-kDa peptides. If the binding and hydrolysis of ATP causes relative movement of the 23- and 50-kDa fragments (Botts et al., 1984), then fluorescent probes near where these two fragments meet could potentially detect the various proposed conformational states. Thus, the M·ADP state would be monitored by the fluorophores reversibly bound, while the pPDM- and V_i-trapped states would possibly reflect the M·ADP·P_i bound states. At the same time, these probes could also reveal conformational differences or similarities between the two trapped states. The two fluorescent probes, DEDA-ADP and MANT-ADP, were chosen because of the sensitivity of their fluorescent moieties to solvent polarity. DEDA-ADP was synthesized with a dansyl group attached with a longer stable leash (see below) to be used in comparison with MANT-ADP, in which the *N*-methylanthraniloyl group is attached directly to the ribose ring. Thus, the different sizes and distances of the fluorphores from ADP could probe different regions of the myosin head.

Synthesis and Characterization of Fluorescent Analogues. We have demonstrated that a new fluorescent derivative of ADP can be prepared by coupling DEDA to the 2′,3′-cyclic carbonate of ADP, generating a base-stable carbamoyl linkage (Scheme I). Base hydrolysis is a potential problem with ester linkages, which are generally employed in the synthesis of ribose-modified fluorescent derivatives (Guillory & Jeng, 1977; Hiratsuka, 1983; Mayer et al., 1984; Schäfer et al., 1986; Williams & Coleman, 1982; Cremo & Yount, 1987). This becomes particularily important in fluorescence studies, where hydrolysis of the ester linkage generates compounds with different fluorescence properties. For example, $Bz_2\epsilon$ADP, a typical ribose-modified ester derivative, shows 5.5% hydrolysis after 14 days at pH 7.0, 4 °C (Cremo & Yount, 1987). In contrast, after analysis of TLC, DEDA-ADP showed no detectable hydrolysis at pH 11.4 for 14 days at 25 °C (detection limit is 0.2% hydrolysis). The approach used here to synthesize DEDA-ADP should be a generally useful method to couple various amines to vicinal diols, generating compounds that are stable under physiological conditions. For example, this methodology has been used to prepare a stable ADP affinity column for S1 (Braxton & Yount, 1987). For the specific purpose here, the synthesis can be easily modified to vary the length of the linker between the ribose ring and the adenine ring. We have also linked fluoresceinamine, an aromatic amine, to ADP, although with lower yields than those reported here for a primary aliphatic amine (Neuron et al., 1988). An alternative approach to prepare stable analogues of this type is to link fluorophores to 2′- or 3′-amino-substituted nucleotides. For example, Eccelston et al. (1987) have prepared a highly effective fluorescent probe by the reaction of fluorescamine with 2′-amino-2′-deoxy-GDP. This approach, however, is limited by the availability of suitable 2′- or 3′-amino-substituted nucleotides.

From our ^{1}H NMR analysis we concluded that DEDA-ADP was a mixture of the 2′- and 3′-isomers in a ratio of 36:67. This mixture of isomers was expected as the nucleophilic amine can cleave at either the 2′ or 3′ side of the cyclic carbonate of ADP. These results were also supported by the finding that the product migrated as a well-resolved doublet on TLC in both solvent systems tested. Our ^{1}H NMR of MANT-ADP showed a 2′/3′ isomeric ratio of 33:66. Similar ratios have been found for a variety of ribose-modified nucleotide analogues with ester linkages (Onur et al., 1983; Schäfer et al., 1986; Mahmood et al., 1987; Cremo & Yount, 1987). Hiratsuka (1983) has previously reported that this analogue is only the 3′-isomer, on the basis of chemical methylation studies that may not accurately reflect the true equilibrium composition.

The apparent equilibrium dissociation constant (K_D) of DEDA-ADP of 1.8 μM with S1 was determined by steady-state polarization as described by Perkins et al. (1984). A Scatchard plot of the data indicated the probe was bound to a single class of sites with a 1:1 stoichiometry (data not shown). This is similar to the results of Watanabe et al. (1981), who reported a dissociation constant for the dansyl-ATP (2′-sulfonamide linkage) to heavy meromyosin of 2 μM. DEDA-ADP was trapped in nearly stoichiometric amounts by pPDM and V_i (Table I); however, trapping was abolished in the presence of excess ADP or in the absence of $MgCl_2$, which indicated that the probe was bound specifically to the active site. The K_D for MANT-ADP, determined by equilibrium dialysis, was 1 μM. As with DEDA-ADP, MANT-ADP bound stoichiometrically to a single class of sites (data not shown). The nearly stoichiometric trapping of MANT-ADP by pPDM and V_i (Table I) was abolished in the presence of excess ADP. These results confirm those of Hiratsuka (1984a), who reported that MANT-ADP was specifically trapped on S1 by V_i in a ratio of 0.88 nucleotide/S1.

Emission Spectra and Quantum Yields. The fluorescence properties of DEDA-ADP were first examined free in buffer

to compare them with the characteristics of other previously synthesized ribose-modified dansyladenosine nucleotide and nucleoside derivatives. These compounds differ in the kind of chemical linkage between the 5-(dimethylamino)-naphthalene-1-sulfonate (or carboxylate) moiety and the ribose ring. A common feature of those derivatives is a low quantum yield in water. The quantum yield of DEDA-ADP (0.089) is similar to that of the 2′-sulfonamide (0.052; Watanabe et al., 1981) and the 3′(2′)-O-ester (0.018, DMAN-ADP; Schäfer et al., 1986). Only the 3′-sulfonic ester (0.21; Skorka et al., 1981) had a notably higher quantum yield. Both dansylic acid (Himel & Mayer, 1970) and 5-[[[(iodoacetyl)amino]ethyl]-amino]napthalene-1-sulfonic acid (Hudson & Weber, 1973) have relative large quantum yields of 0.29 and 0.27, respectively, in aqueous solutions. To reconcile the lower quantum yields of the dansyladenine derivatives, it has been proposed that, in aqueous solutions, the adenine ring statically quenches the naphthoyl moiety (see below). If this is true, then these results indicate that the nature of the linkage between the ribose and the naphthoyl rings can influence the stacking phenomenon. The corrected emission spectrum of DEDA-ADP exhibited a broad unresolved band centered at 578 nm (Figure 3). This large Stokes shift was similar to those of the other dansyl derivatives, which exhibit maxima at 609 nm for the 3′(2′)-O-ester (Mayer et al., 1984) and 554 nm for the 2′-sulfonamide (Watanabe et al., 1981). Again, the exception was the 3′-sulfonic ester with an emission maximum at 516 nm (Skorka et al., 1981).

MANT-ADP has been previously shown to have a relatively high quantum yield in aqueous solution (0.22 at 25 °C; emission maximum 466 nm; Hiratsuka, 1983). Our emission spectrum of MANT-ADP (maximum at 447 nm) and quantum yield (0.255 at 6 °C) are in agreement with these earlier findings. The lifetimes of MANT-ADP (4.06 ns) and DEDA-ADP (3.59 ns) were apparently homogeneous free in solution. The free MANT-ADP our lifetime (4.06 ns, 6 °C) was similar to that of Hiratsuka (1984a) (3.8 ns, 25 °C). However, a single lifetime would not necessarily be expected for a mixture of 2′- and 3′-isomers. Cremo and Yount (1987) showed that the fluorescence of the 2′-isomer of $Bz_2\epsilon$ADP, but not the 3′-isomer, is completely quenched in aqueous solution, possibly by efficient stacking of the 2′-benzoylbenzoyl group with the ethenoadenine ring. As adenine can be a quencher of fluorescence (Scott et al., 1970), it is possible that the single lifetimes of these analogues in aqueous solution were due only to the 3′-isomers.

The effects of reversible binding to S1 upon the fluorescence properties of DEDA-ADP and MANT-ADP were examined to characterize the polarity of the protein environment near the ribose binding site. Hudson and Weber (1973) have shown that, for 5-[[[(iodoacetyl)amino]ethyl]amino]naphthalene-1-sulfonic acid (1,5-AEDANS), as the solvent polarity is decreased the lifetime and the quantum yield increase and the emission maximum blue shifts. Hiratsuka (1983) has also demonstrated for MANT-ADP that there is a small blue shift in the emission maximum and the quantum yield increases with increasing concentration of ethanol or DMF. The fluorescence spectra of both MANT-ADP and DEDA-ADP were blue shifted upon reversible binding to S1 (Figure 3). For MANT-ADP and DEDA-ADP, respectively, we observed a 2.2- and a 2.8-fold increase in quantum yield upon binding to S1 at 6 °C (Table I). These data indicated that both probes were binding to a hydrophobic region of the protein.

The quantum yields of both fluorophores showed a further significant increase of 10–14% upon trapping with either V_i or pPDM. These data indicated that the environment near the ribose binding site was less polar in the trapped states (Table I). However, there was no significant difference between the quantum yields of V_i and pPDM complexes for either fluorophore. For MANT-ADP, we observed a quantum yield of 0.65 in the V_i complex at 6 °C, while Hiratsuka (1984a) reports a quantum yield of 0.35 for MANT-ADP trapped with V_i at 25 °C. This discrepancy may be partially explained by temperature effects on the quantum yield, the possibility of a significant amount of free probe from destabilization of the V_i complex during the measurement at 25 °C, or the presence of nonspecifically bound fluorophore.[2] Consistent with the increase in quantum yield, the emission spectrum of DEDA-ADP exhibited a 2–3-nm blue shift upon trapping with either V_i or pPDM. In contrast, we did not detect a blue shift upon trapping of MANT-ADP (Figure 3) in agreement with Hiratsuka (1984a). These results show that the ribose-modified derivatives can detect a difference between the reversibly bound complexes and the trapped complexes, where trapping causes a decrease in the dielectric constant of the environment around the fluorophores. However, as probes of the polarity of the binding site, the two different trapped states could not be distinguished with either fluorophore.

Lifetimes. The lifetimes of both fluorophores increased but remained homogeneous upon binding to S1 (Table I). As fluorescence lifetimes are a relatively sensitive measure of the heterogeneity of the environment around a fluorophore, homogeneous lifetimes suggested that the analogues were reversibly bound to a single class of sites on S1. This was surprising because both DEDA-ADP and MANT-ADP were shown to be mixtures of 2′- and 3′-isomers, both of which bound to S1 (see Results). These results may suggest that there is enough flexibility between the ribose ring and the fluorescent group that both isomers are forced by hydrophobic interactions into the same binding site on S1. In contrast, it has been shown (Rosenfeld & Taylor, 1984; Cremo & Yount, 1987; Aguire et al., 1989) that the single lifetime of the adenine-modified fluorescent ADP analogue, ϵADP, becomes heterogeneous upon reversible binding to S1, indicating two different enzyme–ligand complexes. Similarily, Shriver and Sykes (1981) using ^{31}P NMR and Trybus and Taylor (1982) using tryptophan fluorescence detected at least two enzyme–ligand complexes for S1·ADP. However, the lifetimes of our ribose-modified probes indicated that they were binding to a single class of sites. Thus, the structural differences between S1–nucleotide complexes that have been measured by other methods were not detected by our ribose-modified probes.

In contrast to the increases in quantum yields upon trapping, we did not observe an increase in the lifetime for either probe upon trapping with V_i or pPDM (Table I). One explanation for this result is a greater effective pK_a of the tertiary amines of both fluorophores in the reversibly bound complex. If the pK_a was then decreased by trapping, a population of nonfluorescent fluorophores would then be deprotonated and become fluorescent. The result would be a net increase in quantum yield with no change in lifetime. A more likely explanation is that the reversibly bound fluorophores are more statically quenched. Chen (1967) has shown that the fluorescence of dansyl amino acid derivatives can be statically

[2] We found that it was necessary to treat the trapped complexes with ATP and EDTA prior to purification by gel filtration, to ensure that nonspecifically bound fluorophore was removed from the protein. Without this treatment, the lifetime studies revealed that there was a significant fluorescence contribution (>15%) from probe that was not bound to the active site.

or dynamically quenched by a number of amino acids including tryptophan, glutamate, and proline. It is likely that MANT-ADP can also be quenched in this way. Thus, although the lifetimes of our probes do not change upon trapping, these data together with the quantum yield data remain consistent with a conformational change in the protein occurring near the ribose binding site upon trapping with either V_i or pPDM.

Aguirre et al. (1989) have shown that the fluorescence decay of ϵADP is altered upon trapping with V_i, resulting in a decrease in the average lifetime from 17.4 to 13.9 ns. However, Perkins et al. (1984) and Cremo and Yount (1987) have shown that the lifetimes of ϵADP remain the same upon trapping with pPDM. These results suggest that there is a difference in the adenine binding site between the pPDM-trapped complex and the V_i-trapped complex. For both of the ribose-modified probes tested here, we did not detect any differences in lifetimes of the V_i- and pPDM-trapped states (Table I). Therefore, the clear differences between the two stable complexes from earlier studies of the adenine binding site cannot be detected with ribose-modified probes, suggesting that the differences are highly localized to the adenine binding pocket.

Polarization. Because only the quantum yields and not the lifetimes of DEDA-ADP and MANT-ADP appeared to reflect differences between the reversibly bound and trapped states, we examined the polarization of the probes as a measure of their mobilities in the various states. From the lifetimes and polarization values of the probes reversibly bound to S1 (Table I) and the limiting polarization values (0.447 for MANT-ADP and 0.437 for DEDA-ADP measured in 95% glycerol at 1 °C; λ_{ex} = 366 nm), the Debye rotational relaxation times of the bound probes may be estimated, with the Perrin (1934) equation. These values, for MANT-ADP (294 ns) and DEDA-ADP (166 ns), indicated that the fluorophores have considerably more motional freedom than if they were rigidly attached to S1 with a rotational relaxation time of about 600ns (Mendelson et al., 1973; Thomas, 1975; 200 ns, if expressed as the rotational correlation time). These data suggest that the two probes have different extents of local motion. DEDA-ADP appears to have more motional freedom, which may reflect that it has a longer linkage between the ribose ring and the fluorophore. The different relaxation times of the two probes may also be explained by the different orientations of the fluorescence emission dipoles relative to the major rotational axes of the protein (Beecham et al., 1986).

Trapping by either pPDM or V_i had little effect on the rotational relaxation times of either probe as the polarization values and lifetimes did not change appreciably (Table I). In contrast, the two different trapped states have been distinguished on this basis with ϵADP. There is no change in the mobility of ϵADP upon trapping with pPDM (Perkins et al., 1984), but the mobility of ϵADP is increased upon trapping with V_i (Aguirre et al., 1989). Thus, as was found for the lifetimes, the differences between the two trapped states that have been previously detected by polarization studies with ϵADP were not detected here with the ribose-modified probes. This suggests that the conformational differences between the two trapped states are localized to the adenine binding site and may not involve the junction region between the 50- and 23-kDa tryptic peptides as we had envisioned.

Accessibility to Solute Quenchers. To determine whether the fluorophores were buried in a hydrophobic pocket or simply immobilized by hydrophobic interactions on the surface of the protein, we examined the accessibility of the fluorophores to solute quenching. For the range of quencher concentrations tested, all Stern–Volmer plots were linear, indicating the probes were bound to a single class of sites. Unfortunately, neither MANT-ADP nor DEDA-ADP was extensively quenched by cesium chloride. Acrylamide was not found to be a particularly effective quencher for either probe, as would be expected for compounds that emit at these relatively long wavelengths (Eftink et al., 1987). The acrylamide constant for MANT-ADP free in solution (2.4 M^{-1}) was similar to the value of 3.2 M^{-1} reported by Hiratsuka (1984a) under slightly different conditions. The potassium iodide and acrylamide quenching constants for MANT-ADP decreased by 12- and 1.7-fold, respectively, upon reversible binding to S1, indicating a decrease in accessibility to the solvent.

The results obtained for DEDA-ADP were more complex. Although the analogue was slightly quenched by the ionic quenchers, the fluorescence was actually enhanced by addition of acrylamide, a relatively hydrophobic molecule. This phenomenon may be partially explained by previous studies, which have shown that aromatic modifications of the ribose ring or phosphate moieties may be more quenched by the adenine ring in aqueous solvents than in solvents of lower dielectric constants (Yarbrough & Bock, 1980; Jacobson & Coleman, 1983; Cremo & Yount, 1987).

The Stern–Volmer plots of both analogues in the trapped complexes were also linear, indicating that the binding sites remained homogeneous. The quenching constants for trapped states remained very small and nearly identical with those for the reversibly bound complexes. There appeared to be no significant difference between the two trapped states for either fluorophore. We found that the accessibility of MANT-ADP dropped 13.5-fold from free to V_i trapped, in agreement with Hiratsuka (1984a), who reported an 11.4-fold drop in the acrylamide quenching constant of MANT-ADP upon trapping with V_i (from 3.2 M^{-1} for free to 0.28 M^{-1} for trapped). In comparison, the solute accessibility of S1·ϵADP decreases by 40% upon trapping with V_i (Rosenfeld & Taylor, 1984) and does not change after trapping with pPDM (Perkins et al., 1984). Taken together, these data indicated that the accessibilities of the two trapped complexes to solvent are different at the adenine binding site but very similar near the ribose binding site.

Nucleotide analogues with modifications on the ribose ring as large as fluorescein (a molecule approximately of 11 × 12 Å; Neuron et al., 1988),[3] can be trapped with either pPDM or V_i on S1. This previously suggested to us that the active site around the ribose ring was unrestricted and perhaps exposed to solvent. In contrast, our quenching data suggest that both MANT-ADP and DEDA-ADP are bound and trapped in a hydrophobic cleft or pocket, not just immobilized by a hydrophobic surface of the protein. This pocket may be an extension of the ATP binding pocket and reflect elements of both the 23- and 50-kDa segments of the heavy chain.

In summary, we have synthesized and characterized a new ribose-modified fluorescent nucleotide analogue, DEDA-ADP, with a base-stable carbamoyl linkage. The previously synthesized MANT-ADP (Hiratsuka, 1983) and DEDA-ADP were used to compare the reversibly bound binary S1 complexes to the stable ternary complexes generated by trapping with V_i or pPDM. Solute quenching studies indicated that both analogues bound reversibly to a single hydrophobic cleft or pocket near the ribose binding site that is relatively inac-

[3] The molecular sizes and distances quoted here were obtained by measuring Corey–Pauling–Koltun space-filling models. The distances between adenine and the fluorophores were measured from the centers of the aromatic rings by assuming the adenine ring was in the anti conformation to the ribose ring.

cessible to solute quenchers. However, polarization measurements indicated that the probes were not completely immobilized. By examining the quantum yields, lifetimes, polarization, and solute accessibility of both probes, we found that the only strong evidence for a conformational change upon trapping with either pPDM or V_i was an increase in quantum yields. In contrast to the results of previous studies with the adenine-modified fluorescent probe ϵADP, the lifetimes of both the binary and ternary complexes with the ribose-modified derivatives were homogeneous, indicating only a single enzyme–ligand complex. In addition, by these fluorescence criteria, we were unable to detect any differences between the V_i and pPDM complexes, indicating that these two states are not structurally different near the ribose binding site. Again, this is in contrast to the fluorescence studies with ϵADP, which show a clear distinction between the adenine binding sites of these two stable complexes. These data taken together suggest that the previously observed spectral characteristics of the adenine binding site in the reversibly bound or stably trapped complexes may be a very short-range local effect that is not transmitted to the region near the ribose binding site that is probed by our nucleotide analogues.

ACKNOWLEDGMENTS

We thank Dr. David Jameson for helpful discussions and for performing the lifetime measurements and Don Appel for acquiring the NMR spectra.

REFERENCES

Adelstein, R. S., & Eisenberg, E. (1980) *Annu. Rev. Biochem. 49*, 921–956.

Aguirre, R., Lin, S. H., Gonsoulin, R., Wang, C. K., & Cheung, H. C. (1989) *Biochemistry 28*, 799–807.

Ajtai, K., Szilagyi, L., & Biro, E. N. A. (1982) *FEBS Lett. 141*, 74–77.

Beecham, J. R., Knutson, J. R., & Brand, L. (1986) *Biochem. Soc. Trans. 14*, 832–839.

Botts, J., Takashi, R., Torgerson, P., Hozumi, T., Muhlrad, A., Mornet, D., & Morales, M. F. (1984) *Proc. Natl. Acad. Sci. U.S.A. 81*, 2060–2064.

Bradford, M. M. (1976) *Anal. Biochem. 72*, 248–254.

Braxton, S., & Yount, R. G. (1988) *Biophys. J. 53*, 178a.

Burke, M., & Knight, P. J. (1980) *J. Biol. Chem. 255*, 8385–8387.

Burke, M., Reisler, E., & Harrington, W. F. (1976) *Biochemistry 15*, 1923–1927.

Chaen, S., Oiwa, K., Shimmen, T., Iwamoto, H., & Sugi, H. (1989) *Proc. Natl. Acad. Sci. U.S.A. 86*, 1510–1514.

Chalovich, J. M., Greene, L. E., & Eisenberg, E. (1983) *Proc. Natl. Acad. Sci. U.S.A. 80*, 4909–4913.

Chen, R. F. (1967) *Arch. Biochem. Biophys. 120*, 609–620.

Cheung, H. C., & Liu, B. M. (1984) *J. Muscle Res. Cell Motil. 5*, 65–80.

Cremo, C., & Yount, R. G. (1987) *Biochemistry 26*, 7524–7534.

DePecol, M. E., & McCormick, D. B. (1980) *Anal. Biochem. 101*, 435–441.

Eccleston, J. F., Gratton, E., & Jameson, D. M. (1987) *Biochemistry 26*, 3902–3907.

Eftink, M. R., Selva, T. J., & Wasylewski, Z. (1987) *Photochem. Photobiol. 46*, 23–30.

Goodno, C. (1979) *Proc. Natl. Acad. Sci. U.S.A. 76*, 2620–2624.

Goodno, C. C. (1982) *Methods Enzymol. 85*, 116–123.

Goodno, C. C., & Taylor, E. W. (1982) *Proc. Natl. Acad. Sci. U.S.A. 79*, 21–25.

Gratton, E., & Limkeman, M. (1983) *Biophys. J. 44*, 315–324.

Gratton, E., Jameson, D. M., & Hall, R. D. (1984) *Annu. Rev. Biophys. Bioeng. 13*, 105–124.

Greene, L. E., Chalovich, J. M., & Eisenberg, E. (1986) *Biochemistry 25*, 704–709.

Guillory, R. J., & Jeng, S. J. (1977) *Methods Enzymol. 46*, 259–288.

Hibberd, M. G., & Trentham, D. R. (1986) *Annu. Rev. Biophys. Chem. 15*, 119–161.

Hiratsuka, T. (1983) *Biochim. Biophys. Acta 742*, 496–508.

Hiratsuka, T. (1984a) *J. Biochem. (Tokyo) 96*, 147–154.

Hiratsuka, T. (1984b) *J. Biochem. (Tokyo) 96*, 155–162.

Hudson, E. N., & Weber, G. (1973) *Biochemistry 12*, 4154.

Huston, E. E., Grammer, J. C., & Yount, R. G. (1988) *Biochemistry 27*, 8945–8951.

Jacobson, M. A., & Colman, R. F. (1984) *J. Biol. Chem. 259*, 1454–1460.

Jameson, D. M., Gratton, E., & Hall, R. D. (1984) *Appl. Spectrosc. Rev. 20*, 55–106.

Kishino, A., & Yanagida, T. (1988) *Nature (London) 334*, 74–76.

Lanzetta, P. A., Alvarez, L. J., Reinach, P. S., & Candia, O. A. (1979) *Anal. Biochem. 100*, 95–97.

Leonard, N. J. (1984) *CRC Crit. Rev. Biochem. 15*, 125–199.

Maeda, M., Patel, A. D., & Hampton, A. (1977) *Nucleic Acids Res. 4*, 2843–2853.

Mahmood, R., Cremo, C., Nakamaye, K. L., & Yount, R. G. (1987) *J. Biol. Chem. 262*, 14479–14486.

Mahmood, R., Elzinga, M., & Yount, R. G. (1989) *Biochemistry 28*, 3989–3995.

Mayer, I., Dahms, A. S., Riezler, W., & Klingenberg, M. (1984) *Biochemistry 23*, 2436–2442.

Mendelson, R. A., Morales, M. F., & Botts, J. (1973) *Biochemistry 12*, 2250–2255.

Neuron, J., Cremo, C., & Yount, R. G. (1988) *Biophys. J. 53*, 179a.

Okamoto, Y., & Sekine, T. (1985) *J. Biochem. (Tokyo) 98*, 1143–1145.

Onur, G., Schäfer, G., & Strotman, H. (1983) *Z. Naturforsch., C: Biochem., Biophys., Biol., Virol. 38*, 49–59.

Parker, C. A., & Reese, W. T. (1960) *Analyst (London) 85*, 587–600.

Penefsky, H. S. (1977) *J. Biol. Chem. 252*, 2891–2899.

Perkins, W. J., Wells, J. A., & Yount, R. G. (1984) *Biochemistry 23*, 3994–4002.

Perrin, F. (1934) *J. Phys. Radium 5*, 497–511.

Reisler, E., Burke, M., & Harrington, W. F. (1974) *Biochemistry 13*, 2014–2022.

Rosenfeld, S. S., & Taylor, E. W. (1984) *J. Biol. Chem. 259*, 11920–11929.

Schäfer, G., Luken, U., & Lubben, M. (1986) *Methods Enzymol. 126*, 683–712.

Scott, T. G., Spencer, R. D., Leonard, N. J., & Weber, G. (1970) *J. Am. Chem. Soc. 92*, 687–695.

Secrist, J. A., III, Barrio, J. R., Leonard, N. J., & Weber, G. (1972) *Biochemistry 11*, 3499–3506.

Shriver, J. W., & Sykes, B. D. (1982) *Biochemistry 21*, 3022–3028.

Skorka, G., Shuker, P., Gill, D., Zabicky, J., & Parola, A. H. (1981) *Biochemistry 20*, 3103–3109.

Stern, O., & Volmer, M. (1919) *Z. Phys. 20*, 183.

Sutoh, K. (1987) *Biochemistry 26*, 7648–7654.

Szilagyi, L., Balint, M., Sreter, F. A., & Gergely, J. (1979) *Biochem. Biophys. Res. Commun. 87*, 936–945.

Taylor, E. W. (1979) *CRC Crit. Rev. Biochem. 6*, 103-164.
Thomas, D. D., Seidel, J. C., Hyde, J. S., & Gergely, J. (1975) *Proc. Natl. Acad. Sci. U.S.A. 7*, 1729-1733.
Trybus, K. M., & Taylor, E. W. (1982) *Biochemistry 21*, 1284-1294.
Wagner, P. D., & Yount, R. G. (1975) *Biochemistry 14*, 1900-1907.
Watanabe, T., Inoue, A., Tonomura, Y., Uesugi, S., & Ikehara, M. (1981) *J. Biochem. (Tokyo) 90*, 957-965.
Wells, C., & Bagshaw, C. R. (1984) *J. Muscle Res. Cell Motil. 5*, 97-112.
Wells, J. A., & Yount, R. G. (1979) *Proc. Natl. Acad. Sci. U.S.A. 76*, 4966-4970.
Wells, J. A., & Yount, R. G. (1982) *Methods Enzymol. 85*, 93-116.
Wells, J. A., Werber, M. M., Legg, J. I., & Yount, R. G. (1979a) *Biochemistry 18*, 4793-4799.
Wells, J. A., Werber, M. M., & Yount, R. G. (1979b) *Biochemistry 18*, 4800-4805.
Williams, N., & Coleman, P. S. (1982) *J. Biol. Chem. 257*, 2834-2841.
Yano-Toyoshima, Y., Kron, S. J., McNally, E. M., Niebling, K. R., Toyoshima, C., & Spudich, J. A. (1987) *Nature (London) 334*, 74-76.
Yarbrough, L. R., & Bock, J. L. (1980) *J. Biol. Chem. 255*, 9907-9911.

Immunochemical Probing of the N-Terminal Segment on Actin: The Polymerization Reaction†

Gargi DasGupta,‡,§ Janet White,‡,§ Martin Phillips,‡,§ Jeannette C. Bulinski,‡,∥,⊥ and Emil Reisler*,‡,§

Molecular Biology Institute, Department of Chemistry and Biochemistry, and Department of Biology, University of California, Los Angeles, California 90024

Received August 23, 1989; Revised Manuscript Received November 27, 1989

ABSTRACT: The N-terminal segment of actin contains a cluster of acidic residues which are implicated in macromolecular interactions of this protein. In this work, the interrelationship between the N-terminal segment and the polymerization of actin was studied by using affinity-purified antibodies directed against the first seven N-terminal residues on α-skeletal actin (SαN). The F_{ab} fragments of these antibodies showed equal affinities for G- and F-actin while the bivalent IgG bound preferentially to the polymerized actin. As monitored by pyrene fluorescence measurements, the binding of F_{ab} to G-actin did not alter the kinetics of the $MgCl_2$-induced polymerization; IgG accelerated this reaction considerably. Consistent with these observations, the binding of F_{ab} to F-actin did not change its morphological appearance in electron micrographs and had no effect on the stability and the rate of dissociation of actin filaments. These results are discussed in terms of their implications to the spatial relationship between the N-terminal segment and the rest of the molecule and in the context of the polymerization reaction of actin in vitro and in vivo.

The regulation of actin polymerization and depolymerization through its interactions with a large number of proteins (Stossel et al., 1985; Pollard & Cooper, 1986) appears central to the function of actin in nonmuscle cell motility. The interest in the molecular mechanism of these interactions has stimulated numerous studies which attempt to map the binding sites between actin and actin-binding proteins (Tellam et al., 1989). A frequent approach in these investigations, initiated by Mornet et al. (1981), was to detect the protein–protein contact sites by cross-linking the protein complexes with carbodiimide. In most cases, such experiments implicated the acidic N-terminal residues on actin in the interactions with actin-binding proteins (Sutoh, 1982; Muneyuki et al., 1985; Sutoh & Mabuchi, 1986; Sutoh & Hatano, 1986; Hambley et al., 1986; Doi et al., 1987). The profound effect that many of these proteins have on the polymerization and depolymerization of actin filaments raises the possibility that the conformation or the net charge of the N-terminal segment influences the formation and stability of F-actin.

A convenient tool for testing the relationship between actin's N-terminus and the polymerization of this protein has become available with the preparation of site-specific antibodies (SαN)[1] directed against the N-terminal segment on actin (Bulinski et al., 1983; Mejean et al., 1986, 1987a; Miller et al., 1987). The SαN antibodies raised against a synthetic peptide corresponding to the first seven N-terminal residues on skeletal α-actin show specific interaction with the N-terminal segment in both monomeric and assembled actin and do not bind to other sites on this protein (Miller et al., 1987). The antibodies completely inhibit actomyosin interactions in the presence of MgATP (DasGupta & Reisler, 1989) but do

† This work was supported by Grant AR22031 from the National Institutes of Health, Grants DMB 85-0857 and DCB 89-40564 from the National Science Foundation, and Grant 877IG2 from the American Heart Association, Greater Los Angeles Affiliate.

‡ Molecular Biology Institute.
§ Department of Chemistry and Biochemistry.
∥ Department of Biology.
⊥ Present address: Department of Anatomy and Cell Biology, Columbia University, New York, NY 10032.

[1] Abbreviations: pyrene-labeled actin, actin modified at Cys-374 with *N*-(1-pyrenyl)iodoacetamide; S-1, myosin subfragment 1; SαN antibodies, peptide antibodies raised against the first seven N-terminal residues of α-skeletal actin; ELISA, enzyme-linked immunosorbent assay; phosphate-buffered saline, phosphate buffer containing 171 mM NaCl, 3.35 mM KCl, 10.1 mM Na_2HPO_4, and 1.84 mM KH_2PO_4, pH 7.4, and, when indicated, 0.05% Tween 20 and 0.1% BSA; SDS-PAGE, sodium dodecyl sulfate–polyacrylamide gel electrophoresis.

0006-2960/90/0429-3319$02.50/0